Development of PGMs alloys suitable for the manufacture of jewelry

Rivoningo E. Chauke [1*], *Rutendo* Matengaifa, *Charles W.* Siyasiya[1] and *Maje* Phasha[2]

[1]Department of Materials Science and Metallurgical Engineering, University of Pretoria, South Africa
[2]Advanced Materials Division, Mintek, South Africa

Abstract. To address the limitations of pure palladium and its alloys in jewelry applications, particularly the insufficient hardness and poor castability, this study investigates novel alloying strategies using both noble and base metals. A minimum hardness of 150 Vickers is essential for wear-resistant jewelry, yet traditional palladium-platinum group metal (PGM) alloys fall short of this benchmark. Using CALPHAD and density functional theory (DFT) methods, the thermodynamic behaviour, phase stability, and mechanical properties of various Pd-based ternary and quaternary systems were analysed. The effects of alloying elements such as Ru, Al, Cu, Ga, and Co were explored in terms of hardness improvement, melting range modification, and structural behaviour. Results revealed that aluminium significantly broadens the melting range and enhances hardness through solid solution strengthening and precipitation. Ru, though limited in solubility, contributes to secondary phase formation and hardness enhancement. A compositionally optimized alloy, PdRu2255, was identified as a promising candidate that satisfies the mechanical, manufacturing, and regulatory requirements for high-quality jewelry applications.

1 Introduction

Palladium (Pd), a platinum group metal (PGM), is increasingly utilized in jewelry due to its white colour, tarnish resistance, and relative affordability compared to platinum (Pt). However, like most pure precious metals, Pd is inherently soft and lacks the mechanical strength required for durable jewelry. To meet industry standards, particularly the minimum hardness threshold of 150 Vickers necessary for acceptable wear resistance, Pd must be alloyed with other elements. Conventional approaches that involve alloying Pd with other PGMs, such as Pt, rhodium (Rh), and iridium (Ir), have shown limited effectiveness in significantly enhancing hardness. Moreover, such alloys tend to exhibit narrow melting ranges and poor fluidity, leading to casting challenges and increased susceptibility to defects [1].

Recent advances in computational materials science have enabled the targeted design of multicomponent alloys by accurately predicting thermodynamic properties and phase

* Corresponding author: u27350097@tuks.co.za

stability. These techniques offer a more efficient alternative to empirical alloy development. In particular, the CALPHAD (CALculation of PHAse Diagrams) method allows for the prediction of phase transformations and solidification behaviour, while density functional theory (DFT) offers atomistic insight into structural and mechanical properties.

This study explores the alloying behaviour of both PGMs and selected base metals, such as aluminium (Al), cobalt (Co), copper (Cu), and gallium (Ga), in 950Pd alloys. The goal is twofold: first, to validate the computational approach by comparing the predicted properties of pure Pd with known experimental data; and second, to identify alloy compositions that not only meet mechanical and casting performance criteria but also comply with jewelry industry regulations for purity and biocompatibility. By integrating CALPHAD and DFT methods, this work aims to design optimized Pd-based alloys capable of delivering superior hardness, improved castability, and overall suitability for high-quality jewelry applications.

2 Platinum group metals (PGMs) alloys for jewelry

Pure precious metals are too soft for most practical applications, making enhanced hardness the primary criterion in selecting alloying elements. In addition to increasing hardness, a suitable jewelry alloy must exhibit good castability, maintain sufficient malleability and colour stability, and be biocompatible [2 - 5]. Any alloying approach must also satisfy the fineness (purity) requirement. Although most platinum group metals (PGMs) share similar physicochemical properties, Ruthenium (Ru) provides a substantial hardness increase in Platinum (Pt) and Pd alloys. This is because Ru possesses a distinct crystal structure compared to other PGMs. Base metals are added to enhance hardness through solid-solution strengthening, precipitate hardening and grain size refinement. Moreover, multicomponent PGM-based alloys have been shown to exhibit superior mechanical properties compared to their binary counterparts [6].

Table 1. Properties of alloying elements commonly used in PGMs alloys [7, 11]

Element	Melting point (°C)	Atomic radii (pm)	Density (cm^{-3})	Modulus (GPa)			Crystal structure	Vickers hardness (Gpa/HV)
				Bulk	Young	Shear		
Pd	1554.8	137	12.023	180	121	44	FCC	0.461/42
Pt	1768	139	21.46				FCC	0.4-0.55
Ru	2333	134	12.44	220	447	173	HCP	2.298
Ir	2446	136	22.56	320	528	210	FCC	1.76
Ga	29.78	135	5.91	NA	NA	NA	NA	
Al	660	143	2.7	76	70	26	FCC	0.167
Cu	1083	128	8.94	140	130	48	FCC	0.369
Co	1495	125	8.83	180	209	75	FCC	1.043

Some of the physical properties of PGMs jewelry alloying elements are shown in Table 1. The atomic radius and crystal structure determine the solid solubilities in Pd. These elements were found to improve the hardness and reduce the melting range as recently studied by Klotz and Held [6]. The effects Cu, Co, Ga, and Al on the melting range was calculated using the CALPHAD method in ThermoCalc as shown in Fig. 1, Ga has the lowest melting point leads to the largest increases in the melting range and lowest solidus whereas Cu contribute the least. Ru has a different crystal structure and makes it less soluble in Pd whereas Al is the most soluble element. Those with high solubility are added for solid solution strengthening and those with limited solubility for precipitate hardening.
In the early development of commercial PGMs jewelry alloys where only Pt-based alloys were used, the only PGMs were used as alloying elements. Three commercially established

regions including the United States of America, Europe, and Japan were marked by their distinct preference for specific alloying elements and precious metal purity; driven by both market taste and fineness regulations [6]. The USA preferred Ir and was flexible in the fineness requirements. However, if Pt was lower than 95wt% pure, the alloying element (Ir) also had to be stamped on the item. Japan preferred Pt-Pd alloys with up to 15wt% of solute species [12]. This was soft hence rhodium plated; in which case the declaration of fineness was voluntary [12]. In Europe, purity was maintained at 95wt% and items were assayed with those below the standard being destroyed. Ru was preferred as an alloying element in Europe [12]. Nonetheless, these alloys were utilized as catch-alls within those markets [12]. Ir is still ubiquitous in many jewelry alloys while Ru is used as a benchmark alloying element for both Pd and Pt. The discussion given below focuses on Ir and Ru and a few select base metals that have been effectively tried and presented in the open literature, namely, Al, Ga, Cu, and Co [2-5].

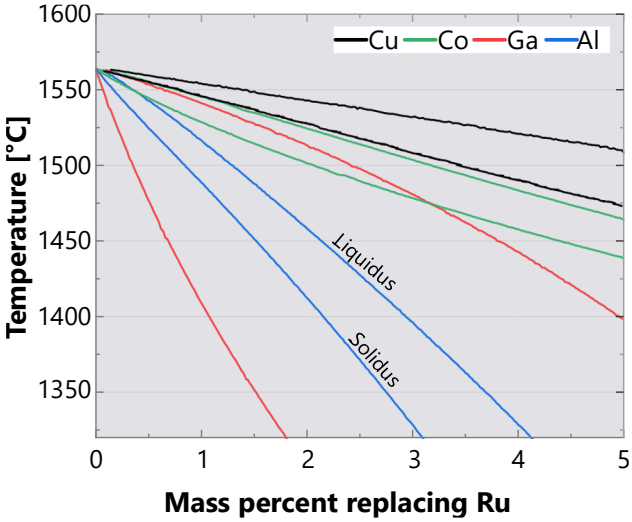

Fig. 1. Effects of the substitution of Ru with a third element on the melting range of 950Pd jewelry alloy [6].

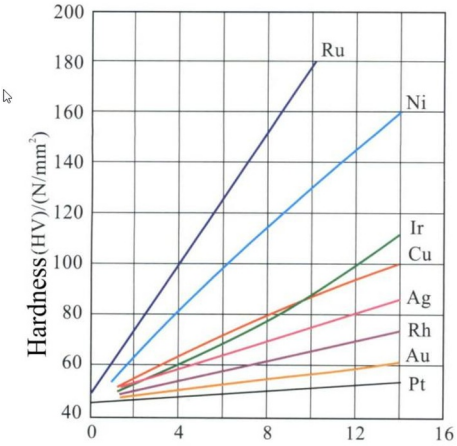

Fig. 2. Effects of alloying elements on the hardness of annealed binary Pd alloys [13].

The obvious reason why early precious metal alloy development stuck to PGMs as alloying elements was driven by limited technological prowess in which case the vacuum

and inert atmospheres could not be created to prevent oxidation of base metals during casting. Today's manufacturing technologies allow for high quality jewelry items despite the challenge of Pd melt's high affinity for oxygen and hydrogen [3].

Fig. 2 shows the effects of alloying elements in heat treated (annealing and ageing) binaries Pd alloys. Among the PGMs, the effects of Pt, Rh, and Ir on hardness are insignificant for practical jewelry purposes whereas Ru can reach up to 120 HV at 5wt%. Pd melt requires a highly controlled atmosphere of the casting chamber when oxidizing base metals are added. Thus, additions of base metals should address the requirement of increasing hardness while preventing the formation of oxides. Nonetheless, base metals can increase the hardness to more than 150 HV required for wear resistance of jewelry pieces.

Ga is also one of the most common solutes in Pd alloys. A hardness of 119 HV for as-cast was reported for addition of 4.5wt% Ga [6]. However, the large melting range allows it to segregate to grain boundaries may cause liquid metal embrittlement [6]. Cu effect is only up to 70HV [13]. Al has been tested by replacing some of the Ru solid solution strengthening of 950Pd and was found to improve the hardness up to content of 1wt%Al, after which the hardness remains constant with more additions [6]. It has also been studied in age hardenable alloy and found to increase the hardness, Fig. 3. The hardness improvement was found to be related to the increase in the precipitation of PdRu precipitates and solid solution strengthening since the Al was completely soluble in 95wt% Pd [14].

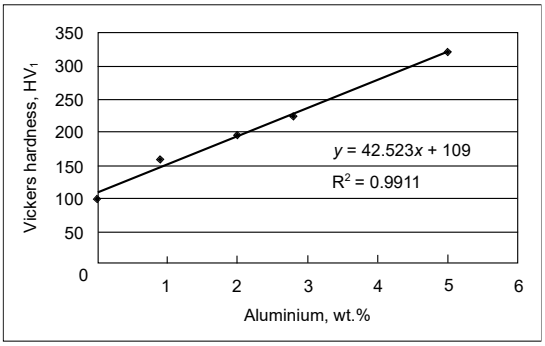

Fig. 3. Variations of the hardness (HV1) with Al content (wt%) of annealed 950PdAl$_x$Ru(5-x) alloys [14]

In Pt, Co was found to yield hardness and tensile strength very similar to Ru and eliminate oxidation and metal-mold reactions in investment casting [15]. It improves the fluidity of Pd alloys and acts as a grain refiner. Studies of Co on Pt alloys found that small additions produced the best result in the elimination of gas porosity [16]. Its notable drawback was ferromagnetism at concentrations of 5wt% and above [16]. All low-melting temperature alloying elements reduce and widen the melting range due to microsegregation, of which Al and Ga have a strong effect [5]. Base metals with melting temperatures higher than Pd are not favoured because they increase the potential for oxidation and may cause melt reactions with the crucible or investment material. Apart from the manufacturing and properties, other elements are excluded because they are volatile, toxic, allergenic (nickel) or radioactive, or too reactive [17]. It is also suggested that highly oxidizing metals should not be added in high concentrations to avoid any possibility of oxidation even if the production chamber's atmosphere is controlled since oxidation affects both fluidity and the colour of finished products [18].

3 Methodology

3.1 ThermoCalc® calculations

The design and optimization of noble element alloys for jewelry and high temperature applications were conducted through the CALPHAD methodology. The CALPHAD comprises a set of mathematical models that describe the thermodynamic properties of phases formed by minimizing the molar Gibbs energy of an alloy with respect to temperature, pressure, and composition differentials [19, 20]. These models are implemented within the ThermoCalc software package. ThermoCalc and TCNOBL3 database for noble metals were used to study the influence of alloying elements on the thermodynamic stability and predict phase transformations and solidification ranges of the Pd-Ru-Al-Co ternary and quaternary systems. The calculations were conducted to help in determining the chemical compositions of the different phases and atomic ratios of the elements involved in solid solution of the matrix. The values of atomic ratios of the elements in the matrix were utilized to conduct DFT first principles calculations to validate stability, determine the lattice constant and ultimately, the mechanical properties of the matrix. Essentially, metallic phases either have random substitution or sublattice solid solution [19, 20]. For multicomponent systems wherein multi-sublattice is often possible, the calculation becomes more complex. Consequently, the concept of lattice stability becomes essential when modeling the Gibbs energy of mixing. The Gibbs energy model is given in equation 1.:

$$G = G^{o} + G_{mix}^{ideal} + G_{mix}^{ex} \tag{1}$$

where G^{o} is the contribution of pure elements, G_{mix}^{ideal} is the Gibbs energy resulting from ideal mixing, and G_{mix}^{ex} is the excess energy resulting from deviation from ideal mixing, which is negative for exothermic mixing and positive for endothermic mixing [19, 20].

For phases with random substitution or single sublattice solid solution, the Gibbs energy model is employed directly, with the assumption that the initial total volume from contributions by each pure component is conserved after mixing [21]. In contrast, for multisublattice phases the sum of excess energies contributions by individual sublattices may be considered for the entire phase.

3.2 DFT calculations

First principle calculations were carried out using the CASTEP code [22] implemented within the Materials Studio software to investigate the structural and elastic properties of pure Pd. The face-centred cubic (FCC) crystal structure of Pd, as illustrated in Fig. 3 was used for the simulations. Electron–ion interactions were described using generalized gradient approximation (GGA) ultrasoft pseudopotentials. A plane-wave cut-off energy of 600 eV and a Monkhorst–Pack k-point grid of 11x11x11 were employed, both of which provided satisfactory convergence for total energy and structural parameters.

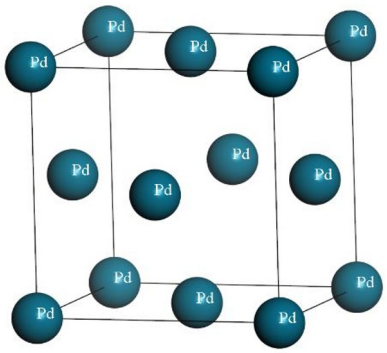

Fig. 3. FCC crystal structure of Pd used for DFT calculations.

4 Results and discussion

4.1 ThermoCalc calculations

Fig. 4(a) shows the pseudo-equilibrium phase diagram at the region above 95PdRuCuAl alloy. Al is varied as a replacement for Ruthenium while Pd and Cu are kept constant at 95 and 0.5wt%, respectively. Generally, Ru increases the melting temperature of Pd in contrast to the combined effect of Al. Therefore, prior to the addition of Al, the liquidus is higher than of pure Pd. The liquidus of the alloy decreases with addition of Al as is always the case for lower melting temperature elements. The liquidus and solidus calculated at 2wt%Al are 1460 and 1418 ºC, respectively. Prior studies have shown that the melting range of 950Pd alloys varies extensively with solute content and type and is very small in the standard 950Pd5Ru and widens for with low melting point elements. The solidification range between 25 and 40ºC may be sufficient as it reduces microsegregation and improves grain structure while also maintaining an acceptable level of fluidity during casting [1, 5]. Fig. 4(b) shows the solidus and liquidus curves of Pd-2.5-Ru-0.5Cu-Al system at fixed Ru and Cu. The melting range is very narrow in 95Pd5Ru and widens with Al addition due to intensified microsegregation.

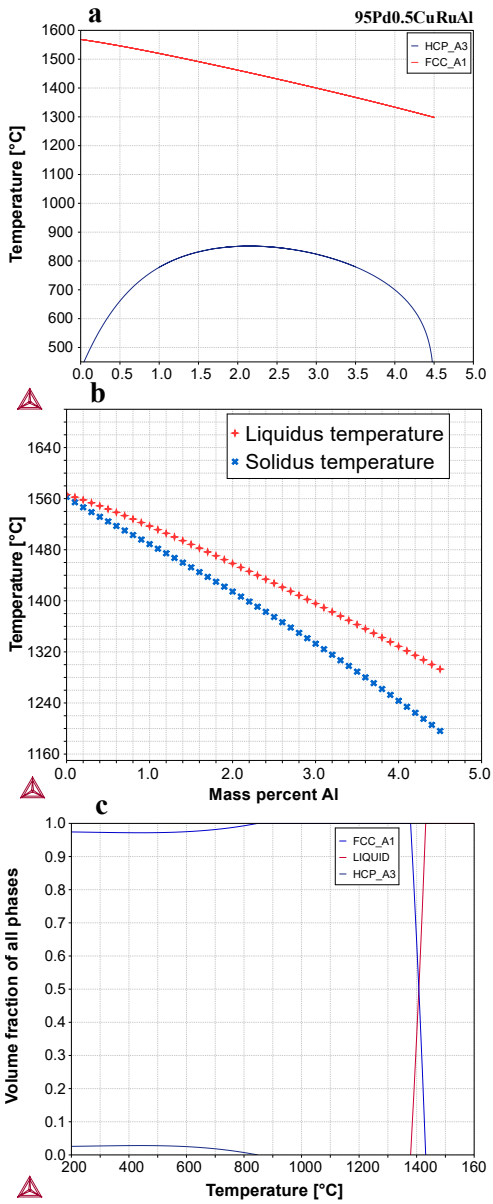

Fig. 4. Thermodynamic psuedo-equilibrium phase diagram and mass fraction-temperature curve of equilibrium phases for the 95PdRuCuAl alloy.

Fig. 4(c) shows the predictions of phase transformation for 2wt%Al i.e., the liquidus, solidus and secondary phase formation temperatures. The quantities of phases and chemical compositions of the matrix and secondary phase and the volume fractions of the matrix are summarized in Fig. 5., taken at 600 ºC. Ruthenium was used as a standard alloying element and further compositional optimization was achieved by additions of Al and Cu, restricted to less than 1wt%. For the current study, the CALPHAD calculations yielded the melting range between 15 ºC for the alloy containing the highest Ru content (3wt%) and 80 ºC for the highest Al content (3wt%). The Solvus indicates unmixing of Pd and Ru at lower temperatures, an important aspect of the age hardening of Pd jewelry alloys.

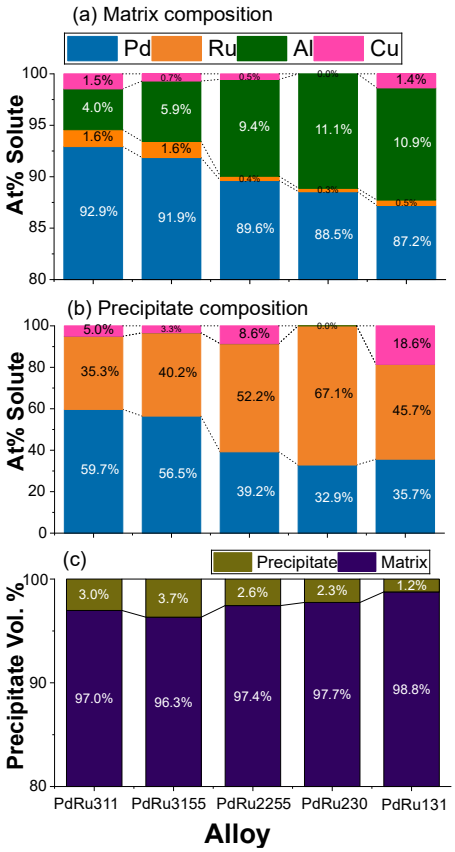

Fig. 6. Summary of ThermoCalc results of (a) composition of the random solid solution matrix, and (b) solid solution secondary phase, and the relative volume fraction of the matrix and secondary phase.

In Fig. 6(a), when Al is increasingly added in the alloy, its solubility of Al gradually increases in the matrix whereas the solubility of Ru decreases. It also can be seen that Al is completely soluble when Pd is 95wt%, while Ru is only fully soluble at high temperature as shown by the appearance of a low temperature secondary phase in Fig. 4 (a & c). Although the content of Cu was kept low, its solubility in the matrix also decreased with Al additions. Fig. 6(b) shows the composition of the secondary phase is Pd(Ru,Cu). Ru gradually becomes dominant and surpasses Pd in the secondary phase as Al is increased. Similarly, Cu shows an increasingly higher solubility in the secondary phase. Cu becomes fully soluble in the matrix when Ru is completely withdrawn, and no secondary phase precipitates as shown for PdRu032 alloy in Fig. 6(c). A high Ru content in the alloy favours a high-volume fraction of the secondary phase. Cu only showed an increase in the composition of the secondary phase but did not have a significant effect on the volume fraction. Generally, Ru increases the melting temperature of 950Pd alloy when added which is in contrast to the combined effect of Al and Cu. The secondary phase has an HCP structure due to Ru which has very limited solubility in Pd.

The potential of producing high quality jewelry from the various alloys to make quality jewelry items was determined by their ability to form sufficient solid solution of the matrix, secondary phase, whilst maintaining the melting range within the acceptable level. The chemical composition matrix was observed to become more binary, being dominated by Pd

and Al. Thus, DFT can potentially best estimate the elastic properties of the matrix. Al also has a large misfit (13%) in Pd; the difference of which can lead to much improved matrix hardness. An assessment of each alloy indicates that PdRu2255 could be the best optimized alloy to fulfil the requirements mentioned above.

4.2 Structural properties of pure Pd from DFT

The Birch–Murnaghan equation of state (Equation 2) [23, 24] describes the behaviour of materials under applied pressure and is commonly used to model the relationship between total energy and volume. It is given by:

$$E(V) = E_o + \frac{9V_oB_o}{16}\left\{\left[\left(\frac{V_o}{V}\right)^{\frac{2}{3}} - 1\right]^3 B_0' + \left[\left(\frac{V_o}{V}\right)^{\frac{2}{3}} - 1\right]^2 \left[6 - 4\left(\frac{V_o}{V}\right)^{\frac{2}{3}}\right]\right\} \quad (2)$$

where E_o is the total energy at equilibrium, V_o is the equilibrium volume, B_o is the bulk modulus, and B_0' is the first derivative of the bulk modulus with respect to pressure.

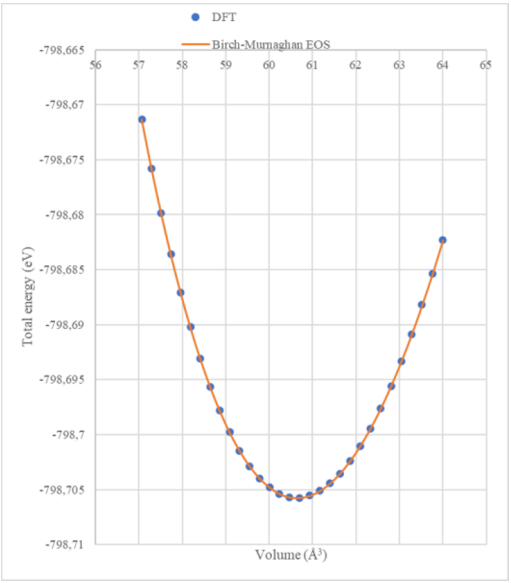

Fig. 7. Plot of total energy versus volume and the Birch – Murnaghan Fit.

Fig. 7 shows the total energy of the Pd unit cell as calculated using DFT, plotted against the unit cell volume (blue dots) in the Birch–Murnaghan equation of state (brown solid line) to determine key parameters: the equilibrium volume (V_0), bulk modulus (B_0), minimum energy (E_0), and the pressure derivative of the bulk modulus (B'_0). The resulting values are listed in **Table 2**. The fit closely matches experimental results, confirming the reliability of the calculations performed using the GGA-PBE exchange–correlation functional [22].

Table 2. Equilibrium lattice parameter, volume, bulk modulus and the pressure derivative from Birch Murnaghan fitting.

	a (Å)	**V_o (Å^3)**	**B_o (GPa)**	**B_o'**	**ρ (g/cm^3)**
This work	3.9287	60.6381	182,4105	5.9	11.64
Experimental	3.8718 (at 4.2K) [28]		180 [13]		12.038 (at 300K) [28]

4.3 Elastic properties of pure palladium from DFT

These mechanical properties are derived from the stress - strain response during the elastic loading. For cubic crystals, there are three independent elastic constants, C_{11}, C_{44}, and C_{12}, from which other elastic moduli can be calculated. These include the bulk modulus (B), shear modulus (G), Young's modulus (E), and additional related properties. The relevant relationships are provided in Equations (2) to (6). Selected calculated values are presented in Table 3 and show good agreement with experimental data, particularly those obtained using the GGA-PBE exchange–correlation functional.

$$B = \frac{1}{3}(C_{11} + 2C_{12}) \tag{3}$$

$$G_V = \frac{1}{5}(C_{11} - C_{12} + 3C_{44}) \tag{4}$$

$$G_R = 5(C_{11} - C_{12})C_{44}[4C_{44} + 3(C_{11} - C_{12})] \tag{5}$$

$$G = \frac{1}{2}(G_V + G_R) \tag{6}$$

$$E = \frac{9GB}{3B} + G \tag{7}$$

Table 3. Formatting sections, subsections and subsubsections.

	PBE	**RPBE**	**PW91**	**WC**	**PBESOL**	**BLYP**	**Experiment**
C_{11}	218.3	199.7	214.1	252.7	260.4	150.7	234.1 [29]
C_{44}	63.9	60.0	60.0	74.5	78.6	35.7	71.2 [29]
C_{12}	162.3	149.9	162.3	188.6	192.3	126.7	176.1 [29]
B	181.0	166.5	179.6	209.9	215.0	134.7	180 [13]
G	49.6	46.0	46.3	57.5	60.8	26.0	44 [13]
E	136.2	126.2	128.0	158.1	166.6	73.4	121 [13]

PBE (Perdew–Burke–Ernzerhof), RPBE (evised Perdew–Burke–Ernzerhof), PW91 (Perdew–Wang 1991), WC (Wu–Cohen), PBESOL (PBE for Solids), BLYP (Becke–Lee–Yang–Parr).

5 Conclusion

This study has demonstrated the potential of computational approaches, specifically CALPHAD and density functional theory (DFT), in the design and optimization of Pd-based alloys for jewelry applications. Traditional Pd-PGM binary alloys fall short in achieving the required hardness and casting properties for practical use. By introducing select base metals such as Al, Co, and Co, it is possible to significantly improve the mechanical performance and widen the melting range, thereby enhancing castability. Among the alloying elements studied, ruthenium proved most effective in increasing hardness through the formation of a

secondary phase, while Al provided solid solution strengthening and improved fluidity due to its complete solubility in Pd. Co additions further enhanced mechanical and casting behaviour, although limited by magnetic properties at higher concentrations. The combination of these effects led to the identification of PdRu2255 as a promising alloy composition that balances hardness, processability, and phase stability within acceptable purity standards.

Ultimately, this work highlights the effectiveness of integrating thermodynamic modelling and atomistic simulations for alloy development, enabling the systematic design of Pd-based jewelry alloys that meet both aesthetic and functional requirements.

References

[1] C. W. Corti, *Basic metallurgy of the precious metals, part II: development of alloy microstructure through solidification and working*, in *Proc. Santa Fe Symp. on Jewelry Manufacturing Technology*, 2008, pp. 03–120.

[2] C. W. Corti, Johnson Matthey Technol. Rev., **66** 4, (2022).

[3] T. Fryé, *Palladium casting: an overview of essential considerations*, The Santa Fe Symposium, Albuquerque, USA (2006).

[4] T. Fryé and J. Fischer-Buehner, *Platinum Alloys in the 21st Century: A Comparative Study*, in *The Santa Fe Symposium on Jewelry Manufacturing Technology*, 2011, pp. 201–230.

[5] C. W. Corti, *Basic metallurgy of the precious metals, part IV: deformation processing, joining and corrosion*, in *The Santa Fe Symposium on Jewelry Manufacturing Technology 2014*, (2014), pp. 111–137.

[6] U. Klotz and F. Held, *Development of new 950Pd investment casting alloys with superior properties*, in *Proc. Santa Fe Symposium on Jewelry Manufacturing Technology*, edited by E. Bell et al., Met., 2019.

[7] L. Pauling, (1947). Atomic radii and interatomic distances in metals. *Journal of the American Chemical Society,* **6**,3, 542–553. https://doi.org/10.1021/ja01195a024

[8] R. E. Bedford, G. Bonnier, H. Maas, and F. Pavese, *Recommended values of temperature on the International Temperature Scale of 1990 for a selected set of secondary reference points*, *Metrologia* **33**, 133 (1996).

[9] C. N. Singman, *Atomic volume and allotropy of the elements*, *J. Chem*. Educ. **61**, 137 (1984).

[10] H. W. King, *Pressure-dependent allotropic structures of the elements*, *Bull. Alloy Phase Diagrams* **4**, 449–450 (1983). https://doi.org/10.1007/BF02868110

[11] PeriodicTable.com, *Vickers hardness values*, https://periodictable.com/Properties/A/VickersHardness.v.log.html (accessed May 2025).

[12] Huckle and D. Schneller, *The development of platinum alloys to overcome production problems*, in *The Santa Fe Symposium on Jewelry Manufacturing Technology*, 1996, pp. 301–326.

[13] J. Maerz and E. Bell, *Platinum alloys: Features and benefits*, in *The Santa Fe Symposium on Jewelry Manufacturing Technology*, 2005, pp. 303–312.

[14] J. Brelle, A. Blatter, and R. Ziegenhagen, *Precious palladium-aluminium-based alloys with high hardness and workability*, *Platinum Met. Rev*. **53**, 189–197 (2009).

[15] C. W. Corti, *The 20th Santa Fe Symposium on Jewelry Manufacturing Technology*, Platinum Met. Rev. **51**, 19 (2007).

[16] C. W. Corti, *Jewellery alloys–past, present and future*, in *The Goldsmiths' Company Jewellery Materials Congress*, 2019.
[17] M. E. Tu and Y. H. Wu, *Multiple allergies to metal alloys*, Dermatol. Sin. **29**, 41–43 (2011).
[18] J. Fischer-Buehner, *The quest for quality: Optimising platinum casting for 21st century needs*, Platinum Met. Rev. **56**, 155–161 (2012).
[19] N. Saunders and A. P. Miodownik, *Thermodynamic models for solution and compound phases*, *in CALPHAD, Calculation of Phase Diagrams*, A Comprehensive Guide, vol. **1**, 1998, pp. 91–126.
[20] L. Kaufman and H. Bernstein, *Computer Calculation of Phase Diagrams* (Academic Press, New York, 1970).
[21] D. A. Porter and K. E. Easterling, *Phase Transformations in Metals and Alloys* (revised reprint) (CRC Press, Boca Raton, 2009).
[22] F.D. Murnaghan, *Proc. Natl. Acad. Sci.* USA **30**, 244 (1944).
[23] F. Birch**,** *Phys. Rev*. **71**, 809 (1947)
[24] J. A. Rayne, *Elastic constants of palladium from 4.2–300 K,* Phys. Rev. **118**, 1545 (1960).